Journal of Enhanced Heat Transfer, 20 (1): 59–71 (2013)

MEASUREMENT AND PREDICTION OF VAPOR-SPACE CONDENSATION OF REFRIGERANTS ON TRAPEZOIDAL-FINNED AND TURBO-C GEOMETRIES

M. A. Kedzierski,[1,*] M. A. Carr,[2] & J. S. Brown[3]

[1]*National Institute of Standards and Technology, Gaithersburg, Maryland 20899, USA*

[2]*Mechanical Engineering Department, U. S. Naval Academy, Annapolis, Maryland 21402, USA*

[3]*Department of Mechanical Engineering, The Catholic University of America, Washington, DC 20064, USA*

[*]Address all correspondence to M. A. Kedzierski E-mail: Mark.Kedzierski@NIST.GOV

This paper reports vapor-space condensation heat transfer measurements for R123, R134a, and R245fa for the integral trapezoidal fin, and the Turbo-CII geometries on vertical plates. The data consisted of heat flux and wall temperature difference measurements. Condensation heat transfer measurements on a smooth plate agreed well with both measurements and predictions from the literature. Overall, the heat transfer performance of the three refrigerants on the trapezoidal fin was within approximately 8 kW/m^2 of one another. Similarly, the condensation heat flux for R134a and R245fa on the Turbo-CII was within approximately 18 kW/m^2 of each other, while the heat flux of R123 on the Turbo-CII was between 10 and 80 kW/m^2 less than that of R245fa. An existing finned tube condensation model was modified to be expressed in terms of the gradient of the condensate curvature with respect to the length of the liquid–vapor interface. Curvature gradients for the two surfaces were developed that, when substituted into the modified model, predicted the present measured driving temperature differences for the trapezoidal fin and the Turbo-CII to within 0.4 and 1.2 K, respectively, for all measurements except for R123 on the Turbo-CII surface. With the aid of the curvature gradients, simple models were developed to predict the performance of the trapezoidal, low-finned tube, and the Turbo-C tube. The heat flux to the low-finned tube and the Turbo-C tube were predicted to within 10% and 15%, respectively, of the measured values from the literature for four different fluids.

KEY WORDS: *enhanced heat transfer, low-finned tube, passive enhancement, R123, R134a, R245fa, Turbo-CII*

1. INTRODUCTION

Despite the rigors of ozone (Montreal Protocol, 1987) and climate (Kyoto Protocol, 1997; European Mobile Directive, 2006) policies, both R134a and R123 remain viable refrigerants for use in chillers and other refrigeration and air-conditioning equipment. According to Calm (2012), R123 still maintains nearly 40% of the global centrifugal chiller market share. Calm (2012) also states that "R134a is now the most widely used single-compound refrigerant in new equipment on a worldwide basis." Considering this and that the US Clean Air Act permits the manufacture of R123 chillers up to the end of 2019 and that the production of R134a is not currently planned to be phased out [Copenhagen Amendment (1992) to the Montreal Protocol (1987)], the study of the vapor-space condensation heat transfer characteristics of these refrigerants is essential for promoting efficient systems. R245fa is also an important refrigerant to study being that it has a 100-year time horizon global warming potential (GWP) that is 39% less than that of R134a (IPCC, 2007). Brown (2012) illustrates that further reduction in GWP is possible by creating blends of more traditional refrigerants with low-GWP refrigerants, including flammable ones.

1065-5131/13/$35.00

NOMENCLATURE

A	surface area, (m)
B	regression constant, (Table 1)
c_b	fraction of the tube circumference flooded by condensate
C	regression constant, [Eqs. (1)–(3)]
D	diameter, (m)
e	fin height, (m)
e_v	effective mean vertical fin height, (m)
g	gravitational constant, (m/s^2)
i_{fg}	latent heat of condensation, (kJ/kg)
k	thermal conductivity, (W/m · K)
L_g	condensing length influenced by gravity, (m)
L_s	condensing length influenced by surface tension, (m)
L_y	length of test surface in y direction, (m)
p_f	fin pitch, (m)
P	pressure, (kPa)
q''	average wall heat flux, (W/m^2)
s	coordinate along fin arc with origin at the fin tip, (m)
S_r	spacing between the fins at the fin root, (m)
t	width of fin, (m)
T	temperature, (K)
T_s	temperature of the saturated vapor, (K)
T_w	temperature of surface at root of fin, (K)
u_i	standard uncertainty
U	expanded uncertainty
U_{Tw}	expanded uncertainty in the wall temperature, (K)
$U_{q''}$	relative expanded uncertainty, (%) in heat flux measurement
x	test surface coordinate
y	test surface coordinate

Greek Symbols

ΔT_s	wall temperature difference: $\Delta T_s = T_s - T_w$, (K)
κ	curvature, (m)
μ	dynamic viscosity, (kg/m · s)
ρ	density, (kg/m^3)
σ	surface tension, (N/m)
ξ	dimensional constant set to 1 m in Eq. (12)

Subscripts

f	fin side
l	liquid
o	over the fins
p	projected
r	at the fin root
s	saturated liquid or vapor state
t	fin tip
v	vapor

Low-GWP blends with R134a, and R245fa will necessitate the evaluation of the heat transfer performance of these fluids for some time to come, e.g., as is done by Cavallini et al. (2010) for condensation and Brown et al. (2012) for flow boiling.

Vapor-space condensation measurements and predictions for R123, R134a, and R245fa on conventional passively enhanced condenser tube geometries can contribute greatly to the efficient design of new refrigeration and air-conditioning equipment for these fluids. Park et al. (2010) have contributed to this effort by providing baseline measurements for condensation heat transfer of all the above fluids plus that of R22 on a smooth, horizontal tube. Based on their measurements, they concluded that R245fa appeared to be a long-term replacement for R123. Jung et al. (1999) examined the condensation heat transfer performance of R123 and R134a on a trapezoidal finned tube and a Turbo-C[1] tube. They found that the condensation heat transfer coefficient for the Turbo-C tube was as much as eight times greater than that for a smooth tube, thus, illustrating the potential for the Turbo-C for facilitating thermodynamically efficient system designs.

Models for predicting the condensation heat transfer performance on finned tubes inevitably require the consideration of surface-tension drainage of condensate from the fins. Honda and Nozu (1987), Adamek and Webb (1990), Rose (1994), and Webb et al. (1985) have all de-

[1]Certain commercial equipment, instruments, or materials are identified in this paper in order to specify the experimental procedure adequately. Such identification is not intended to imply recommendation or endorsement by the National Institute of Standards and Technology, nor is it intended to imply that the materials or equipment identified are necessarily the best available for the purpose.

veloped condensation heat transfer models that include surface tension effects. One of the more successful models, due to its simplicity and accuracy, is that of Rose (1994). He developed a model based upon dimensional analysis, which is able to provide a simple way to predict the heat transfer performance of a particular class of enhanced tubes. These models are limited to the prediction of the performance of vapor-space condensation on the trapezoidal fin geometry and are unable to predict either the Turbo-C or Turbo-CII geometries.

The focus of the present study is to provide experimental data and a model to document and to predict the relative performance of R123, R134a, and R245fa on two heat transfer surfaces: trapezoidal low-fin and Turbo-CII. The measurements were done on vertical plates rather than round, horizontal tubes in order to isolate and study the effects of the fin condensation without the effects of condensate retention, which is a characteristic associated with horizontal tubes. The measurements on plates were designed to allow for the development of a predictive model for condensation on the trapezoidal, low-finned and the Turbo-CII geometries on vertical plates and horizontal tubes.

2. APPARATUS

Figure 1 shows a schematic of the apparatus that was used to measure the vapor-space condensation heat trans-

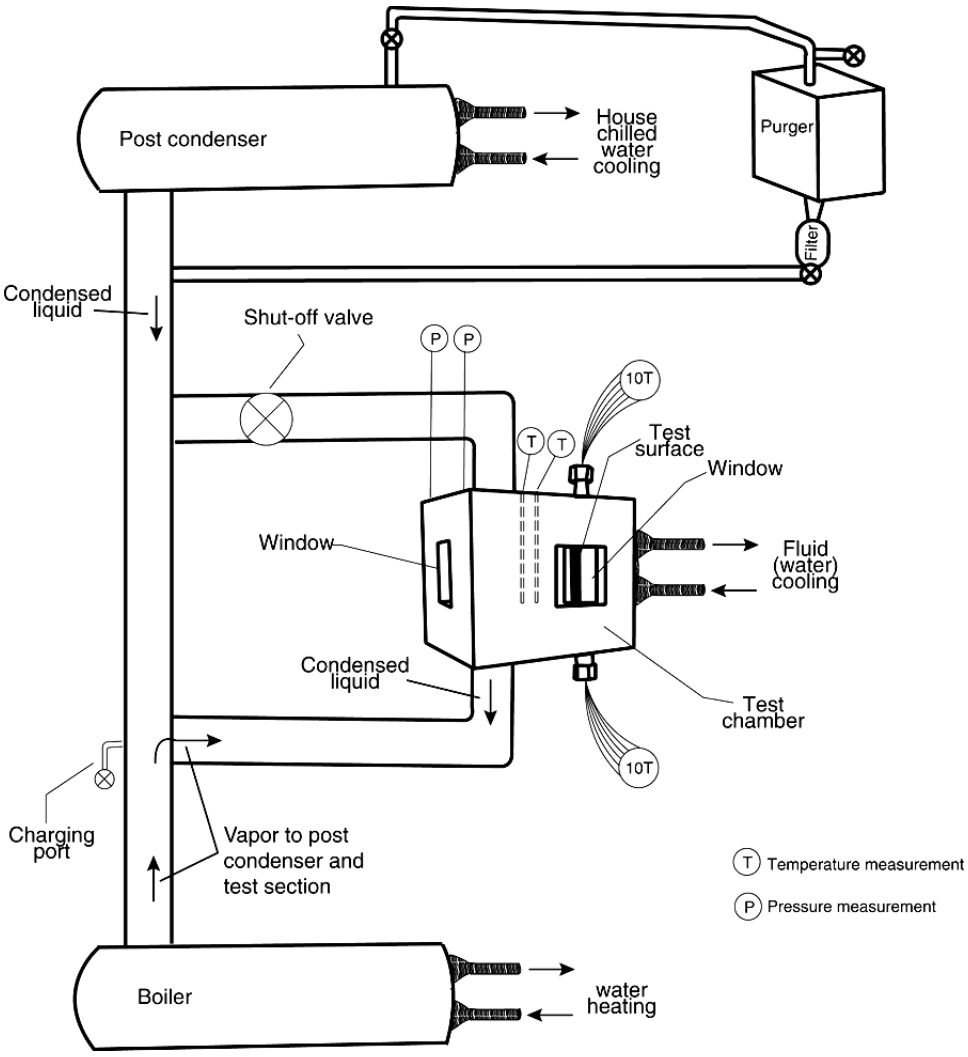

FIG. 1: Condensation test apparatus.

fer for the test surfaces. Specifically, the apparatus was used to measure the vapor saturation temperature (T_s), the average condensation heat flux (q''), and the wall temperature (T_w) of the test surface at the fin root. The three principal components of the apparatus were the test chamber, the postcondenser, and the boiler. The internal dimensions of the test chamber were approximately 254 $\times$ 200 $\times$ 130 mm. The boiler contained approximately 10 kg of refrigerant. Hot building water flowing inside the boiler tubes heated the test refrigerant on the shell side. The test section was visible through three, flat quartz windows. High-velocity (2.5 m/s) water cooled the opposing side of the finned condensing test surface. Varying the cooling water temperature varied the heat flux. The vapor produced by the boiler was condensed by the postcondenser and the test section and it was returned by gravity to the liquid pool. The postcondenser was identical to the shell-and-tube boiler; however, chilled water flowed inside the tubes while the vapor condensed on the outside of the tubes. The duty of the boiler and the postcondenser were significantly large so that a wide variation in the duty of the test surface would not affect the saturation pressure of the test apparatus. The purger and the desiccant filter removed noncondensable gases and water, respectively, from the test refrigerant after charging and before testing.

To reduce errors associated with the saturation temperature measurement, two 450 mm long 1.6 mm diameter stainless steel sheathed thermocouples were used to measure the vapor saturation temperature. The small thermocouple bead diameter provided for a relatively rapid response time. Approximately 180 mm of each thermocouple length was exposed to the vapor of the test chamber. The portion of each thermocouple that was in the test chamber was shielded with a 6 mm diameter stainless steel tube and was in contact with the saturated refrigerant vapor. The tips of the two thermocouples were placed near the lower edge of the test plate and approximately 60 and 95 mm, respectively, from the plate face.

2.1 Test Surfaces

Figure 2 shows the cross section of the oxygen-free high-conductivity (OFHC) copper integral-trapezoidal-fin test

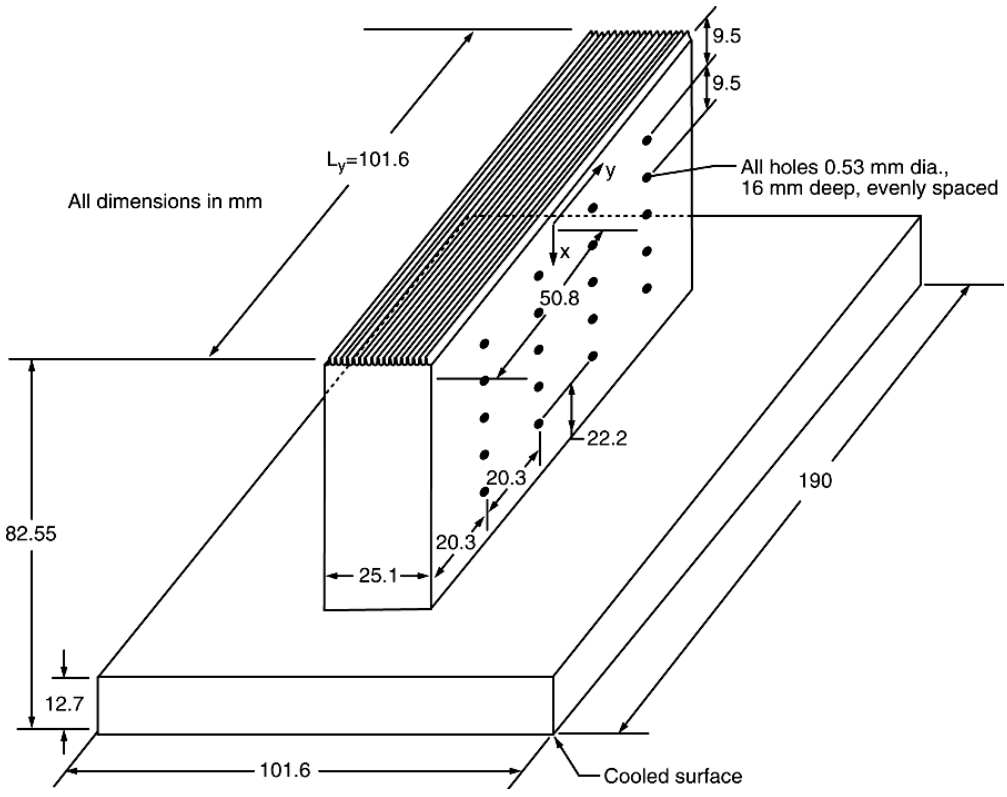

FIG. 2: OFHC copper trapezoidal-fin test plate and thermocouple coordinate system.

plate used in this study. The integral-trapezoidal-fin surface was machined directly onto the top of the test plate by electric discharge machining (EDM). The total length of the plate (L_y) was approximately 101 mm. As shown in Fig. 3, the surface had a fin pitch (p_f) of approximately 1.36 mm giving nominally 746 fins per meter oriented along the long axis of the plate. The fin-tip width (t_t), the fin height (e), and the spacing between the fins at the fin root (S_r) were approximately 0.24, 1.53, and 0.88 mm, respectively. The ratio of the surface area to the projected area of the surface was 2.87. If the delineation between the fin and the fin root is defined as where the fin curvature changes from convex to concave, then the ratio of the fin area to projected area (A_f/A_p) and the ratio of the root area to the projected area (A_r/A_p) was approximately 1.65 and 1.11, respectively.

Figure 3 shows a top and a side view of the notched, saw-toothed fins of the Turbo-CII surface. There are nominally 1575 fins per meter with a fin-tip width (t_t), the fin height (e), and the spacing between the fins at the fin root (S_r) was approximately 0.12, 0.74, and 0.51 mm, respectively. The Turbo-CII surface was unrolled from a section of 25.25 mm diameter tube with the inner surface machined flat. The unrolled section was soldered onto a copper test plate. The material properties of the fins and base tubing, the test plate, and the intervening solder layer were all accounted for in measuring the heat flux and surface temperature in the same manner as done in Kedzierski (1995).

3. MEASUREMENTS AND UNCERTAINTIES

The standard uncertainty (u_i) is the positive square root of the estimated variance. The individual standard uncertainties are combined to obtain the expanded uncertainty (U), which is calculated from the law of propagation of uncertainty with a coverage factor. All measurement uncertainties are reported at the 95% confidence level except where specified otherwise. For the sake of brevity, only a summary of the basic measurements and uncertain-

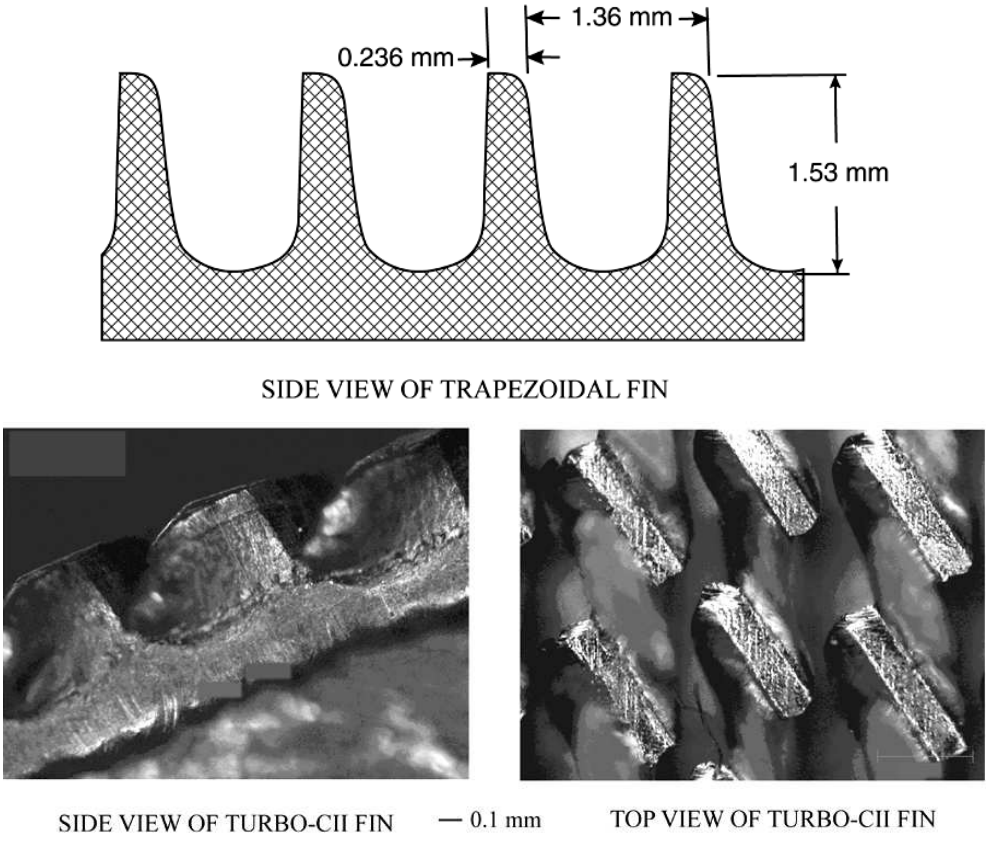

FIG. 3: Trapezoidal-fin and Turbo-CII fin geometries.

ties is given below. Complete detail on the heat transfer measurement techniques and uncertainty estimates can be found in Kedzierski (2000) and in Carr (2002).

All of the copper–constantan thermocouples and the data acquisition system were calibrated against a glass-rod standard platinum resistance thermometer (SPRT) and a reference voltage to a residual standard deviation of 0.005 K. Considering the fluctuations in the saturation temperature during the test and the standard uncertainties in the calibration, the expanded uncertainty of the average saturation temperature was no greater than 0.04 K. Consequently, it is believed that the expanded uncertainty of the temperature measurements was less than 0.1 K.

Twenty 0.5 mm diameter thermocouples were force fitted into the wells of the side of the test plate shown in Fig. 2. The heat flux and the wall temperature were obtained by regressing the measured temperature distribution of the block to the governing two-dimensional conduction equation (Laplace equation). In other words, rather than using the boundary conditions to solve for the interior temperatures, the interior temperatures were used to solve for the boundary conditions following a backward stepwise procedure given in Kedzierski (1995). As shown in Fig. 2, the origin of the coordinate system was centered on the surface with respect to the y direction at the heat transfer surface. Centering the origin in the y direction reduced the uncertainty of the wall heat flux and temperature calculations by reducing the number of fitted constants involved in these calculations.

Fourier's law and the fitted constants from the Laplace equation were used to calculate the average heat flux (q'') normal to and evaluated at the heat transfer surface based on its projected area.[2] The average wall temperature (T_w) was calculated by integrating the local wall temperature (T). The driving wall temperature difference was calculated from T_w and the measured temperature of the saturated vapor (T_s). Considering this, the relative expanded uncertainty in the heat flux ($U_{q''}$) was greatest at the lowest heat fluxes, approaching 8% of the measurement near 2 kW/m^2. In general, the $U_{q''}$ remained less than 4% for heat fluxes greater than 20 kW/m^2. The average random error in the wall superheat (U_{Tw}) remained between 0.01 and 0.10 K with an average value of approximately 0.04 K. Plots of $U_{q''}$ and U_{Tw} versus heat flux can be found in Carr (2002).

[2]All heat fluxes presented in this manuscript are based on the projected area.

4. EXPERIMENTAL RESULTS

The heat flux was varied from approximately 65 to 2 kW/m^2 for the trapezoidal surface and from 110 to 2 kW/m^2 for the Turbo-CII surface. The saturation temperature was 313.15 K for all of the vapor-space condensation tests. Almost no condensate retention was observed on the surface for all test heat fluxes. The dimensionless liquid–vapor interfacial shear stress as defined by Rohsenow et al. (1956) was estimated to be less than 1.4×10^{-4} for all of the data. Data were taken, on average, over six days for each fluid and test plate resulting in a total of 491 measurements. Carr (2002) tabulated the measured heat flux and wall temperature difference for all of the data.

The heat transfer measurements were qualified by measuring the rate of R134a condensation on a vertical-smooth plate and comparing the results to the Nusselt (1916) solution. Figure 4 shows the measured heat flux (q'') versus the measured driving temperature difference ($\Delta T_s = T_s - T_w$) for R134a together with the predicted heat flux and temperature difference. The largest deviation of the measured q'' and ΔT_s from the Nusselt (1916) solution for laminar filmwise condensation is approximately 10%, with better agreement at the lower q''. The measured heat fluxes at the larger ΔT_s were larger than those predicted by the Nusselt solution, which is consistent with the heat transfer enhancing effects of larger film Reynolds numbers that are not accounted for in the Nusselt solution. In addition, the R134a condensation measurements of Jung et al. (1999) on a 19 mm diameter, smooth, horizontal tube are within 15% of the present

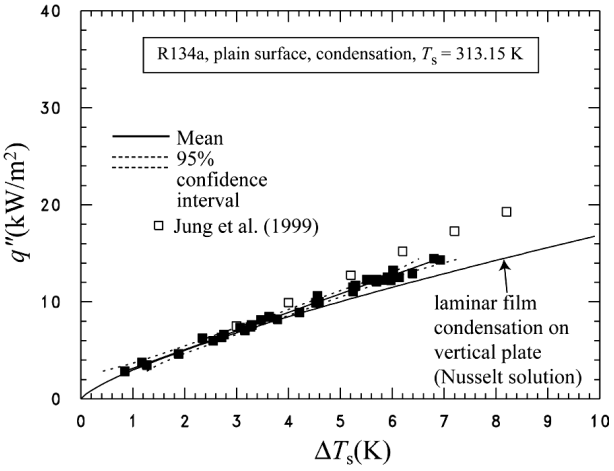

FIG. 4: Condensation heat flux versus driving temperature difference for R134a on a vertical plain surface.

measurements on a vertical-smooth plate. A Nusselt-type analysis predicts that for the same driving temperature difference, the heat flux on a 101 mm long vertical plate should be approximately 2% larger than that for a 19 mm diameter, horizontal tube (Incropera and DeWitt, 2002).[3]

Figures 5 and 6 show the measured heat flux versus ΔT_s for the various fluids for the trapezoidal fin and the Turbo-CII surfaces, respectively. The solid lines are a cubic best-fit regression of the data. Table 1 gives the constants for the cubic regression of the wall temperature difference versus the heat flux for each fluid and surface tested. The dashed lines, to either side of the mean, represent the lower and upper 95% simultaneous (multiple-use) confidence intervals for the mean.

[3] $q''_{\text{Plate}}/q''_{\text{tube}} = 1.13/0.728\,(L_y/D)^{1/4}$.

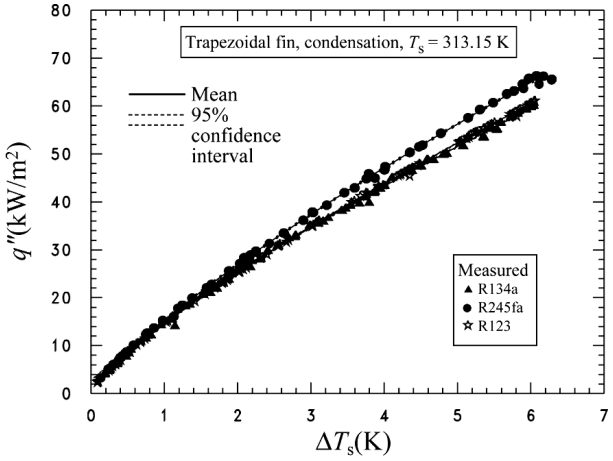

FIG. 5: Measured condensation heat flux versus driving temperature difference for R134a, R245fa, and R123 on a trapezoidal surface.

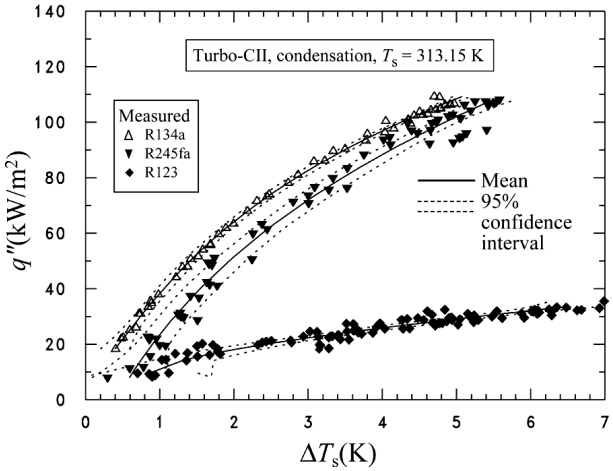

FIG. 6: Measured condensation heat flux versus driving temperature difference for R134a, R245fa, and R123 on a Turbo-CII surface.

Figure 5 shows the condensation heat transfer measurements for R123, R134a, and R245fa on the vertical, trapezoidal surface. The heat flux for R245fa is approximately 10% greater than that for R134a at the same driving temperature difference. The condensation curves for R123 and R134a are nearly identical and are within the measurement uncertainty for most of the data.

The heat flux for the trapezoidal fin surface proved to be relatively insensitive to test fluid, being within approximately 6 kW/m^2 of each fluid run for the same driving temperature difference. The residual standard deviation of the regressions—representing the proximity of the data to the mean—for both fluids was approximately 0.025 K. The expanded uncertainty of the estimated mean wall temperature difference for the three fluids on the trapezoidal surface was approximately 0.015 K.

Figure 6 shows the condensation heat transfer measurements for R123, R134a, and R245fa on the vertical, Turbo-CII surface. For R134a and R245fa, the heat flux for the Turbo-CII surface is approximately double that of the trapezoidal-fin surface for the same driving temperature difference. For driving temperature differences greater than 3 K, the heat flux for R134a on the Turbo-CII is approximately 10 kW/m^2 greater than that for R245fa, which is nearly the reverse relative performance of the two fluids on the trapezoidal surface. The R123 heat flux is between 10 and 80 kW/m^2 less than that of R245fa. The poorer performance of R123 on the Turbo-CII surface may be due to the combined effects of a larger liquid density and a larger surface tension than that of R134a and R245fa at the present test temperature. For the vertical plate, the larger liquid density encourages gravity to work against surface-tension drainage on the fins. Likewise, the long condensing length of the plate (L_s) gives the opportunity for the larger surface tension to induce partial flooding of the fin surface. Both of these effects work to reduce condensation heat transfer. The residual standard deviations of the regressions for R123, R134a, and R245fa were approximately 0.025, 0.025, and 0.05 K, respectively. The expanded uncertainties of the estimated mean wall temperature differences for R123, R134a, and R245fa on the Turbo-CII surface were approximately 0.015, 0.015, and 0.03 K, respectively.

TABLE 1: Constants for cubic condensation fits $\Delta T_s = B_0 + B_1 q'' + B_2 q''^2 + B_3 q''^3 \Delta T_s$ in Kelvin and q'' in W/m^2

Fluid	B_0	B_1	B_2	B_3
R123 & trapezoidal fin 0.1 K $\leq \Delta T_s \leq$ 6.0 K	–7.58 $\times 10^{-02}$	6.17 $\times 10^{-05}$	9.20 $\times 10^{-10}$	–4.66 $\times 10^{-15}$
R134a & trapezoidal fin 0.2 K $\leq \Delta T_s \leq$ 6.0 K	–5.35 $\times 10^{-02}$	4.73 $\times 10^{-05}$	1.23 $\times 10^{-09}$	–7.65 $\times 10^{-15}$
R245fa & trapezoidal fin 0.3 K $\leq \Delta T_s \leq$ 6.5 K	–1.65 $\times 10^{-01}$	6.28 $\times 10^{-05}$	3.76 $\times 10^{-10}$	8.09 $\times 10^{-17}$
R123 & Turbo-CII^{TM} 1.0 K $\leq \Delta T_s \leq$ 6.0 K	1.45	–1.87 $\times 10^{-04}$	1.43 $\times 10^{-08}$	–1.28 $\times 10^{-13}$
R134a & Turbo-CII^{TM} 0.3 K $\leq \Delta T_s \leq$ 5.0 K	–1.04 $\times 10^{-02}$	2.83 $\times 10^{-05}$	–7.82 $\times 10^{-11}$	2.31 $\times 10^{-15}$
R245fa & Turbo-CII^{TM} 0.7 K $\leq \Delta T_s \leq$ 5.9 K	4.00 $\times 10^{-01}$	2.32 $\times 10^{-05}$	9.64 $\times 10^{-11}$	1.16 $\times 10^{-15}$

5. ROSE MODEL

Rose (1994) developed a simple model to predict condensation heat transfer on low, integral-finned tubes by building an area-weighted average model for the different regions of the tube. Expressions for the condensation heat flux for fin tip (q''_t), the fin side (q''_f), and the space between the fins at the fin root (q''_r) are arrived at by dimensional analysis while imposing consistency with traditional solutions for laminar film condensation such as those given in Incropera and Dewitt (2002):

$$q''_t = \left\{ \frac{\rho_l i_{fg} k_l^3 \Delta T_s^3}{\mu_l} \left(\frac{C_t^4 \Delta\rho g}{D_o} + \frac{0.143\sigma}{t_t^3} \right) \right\}^{1/4} \quad (1)$$

$$q''_f = \left\{ \frac{\rho_l i_{fg} k_l^3 \Delta T_s^3}{\mu_l} \left(\frac{C_f^4 \Delta\rho g}{e_v} + \frac{0.143\sigma}{e^3} \right) \right\}^{1/4} \quad (2)$$

$$q''_r = \left\{ \frac{\rho_l i_{fg} k_l^3 \Delta T_s^3}{\mu_l} \left(\frac{C_r^4 \Delta\rho g}{D_r} + \frac{0.143\sigma}{S_r^3} \right) \right\}^{1/4} \quad (3)$$

The constants C_t and C_f are the ones traditionally used for the condensation heat transfer coefficient on horizontal tubes (C_t = 0.728) and vertical, flat plates (C_f = 0.943), respectively. Rose (1994) modifies the coefficient for horizontal tubes in order to calculate a proper average condensation rate at the fin root; however, it is assumed here that $C_r = C_t$ for vertical plates. The e_v is the effective mean vertical fin height, as defined by Rose (1994), and is equal to L_y for a vertical plate.

The fluid properties of the condensate are evaluated at saturated conditions including the liquid density (ρ_l), the liquid thermal conductivity (k_l), the dynamic liquid viscosity (μ_l), the surface tension (σ), and the difference between the liquid and vapor densities ($\Delta\rho$). The latent heat of vaporization is i_{fg}, and g is the gravitational constant.

The total condensation heat flux (q'') of the tube based on the projected area (A_p) is

$$q'' = (1 - c_b) \left(\frac{A_t}{A_p} q''_t + \frac{A_f}{A_p} q''_f + \frac{A_r}{A_p} q''_r \right) \quad (4)$$

Here, c_b is the fraction of the tube circumference that is flooded by condensate, which is practically inactive for condensation heat transfer (Rudy and Webb, 1985). A simplified form of c_b for trapezoidal fins by Rudy and Webb (1985) is

$$c_b = \frac{1}{\pi} \cos^{-1} \left(1 - \frac{4\sigma}{\rho_l g D_o S_r} \right) \quad (5)$$

The above model, i.e., Eq. (4), for the total heat flux differs from that provided by Rose (1994) in that the Rose model does not discount the fin-tip heat transfer in the flooded region. In addition to accounting for a loss of heat transfer in the flooded region, the Rose model also accounts for a reduction of condensation in the fin-side and fin-root areas due to partial flooding in the active region of the tube.

For the analysis in this paper for vertical plates, condensate flooding is neglected by setting c_b equal to zero. This is approximately true due to the drainage strip on the end of the plate to discourage condensate flooding there. In addition, both the tube diameter at the root of the fin

(D_r) and the tube diameter over the fins (D_o) are taken as the total length of the plate, L_y. The resulting predictions with the modified Rose model for the vertical plate are shown in Fig. 7. The predicted heat flux is roughly 5% to 25% less than the measured heat flux for the three test fluids. Considering this, the Rose model does a good job of capturing the physics and predicting the condensation of the integral-finned trapezoidal surface.

6. MODEL DEVELOPMENT

The methodology for developing models to predict near-zero shear condensation on trapezoidal, low-finned and Turbo-CII or Turbo-C geometries is to, first, rearrange Rose's model in terms of the liquid–vapor interface curvature gradient of the condensate film. The second step is to develop expressions for the condensate curvature gradient[4] from the heat transfer measurements of the vertical plates. The vertical plate measurements are not confounded by condensate retention; therefore, the heat transfer to the fin can be isolated more so than for a horizontal tube. The final step is to rebuild the model for the tube using the new curvature gradients while accounting for loss of heat transfer due to condensate retention.

Zener and Lavi (1974) proposed a condensation surface with a constant pressure gradient (dP/ds) along the arc length of the condensate's liquid–vapor interface (s). For low fins and thin films, this pressure gradient can be approximated by the gradient in curvature of the liquid–vapor interface of the condensate film as

$$\frac{dP}{ds} = \sigma \frac{d\kappa}{ds} \tag{6}$$

The condensation heat flux for such a surface, while including the component of gravity forces in the s direction ($\rho_l g_s$), and neglecting the condensate film thickness at s = 0, can be written as

$$q'' = \left(\frac{\rho_l i_{fg} k_l^3 \Delta T_s^3}{\mu_l}\right)^{1/4} \left(\frac{\rho_l g_s + \sigma \left|\frac{d\kappa}{ds}\right|}{4L_s}\right)^{1/4} \tag{7}$$

where L_s is the condensing length, i.e., the total length over which the condensate drainage force acts.

The Rose (1994) model is nearly identical to the constant pressure gradient model with the exception that the gravity and surface tension terms do not share the same denominator (condensing length) as for the Zener and Lavi (1974) model. The advantage of the above equation is that it can be seen that the gradient of the condensate curvature can be used to tailor Rose's model to other geometries, including the Turbo-CII.

Using Eq. (7) as a guide, the general form of Rose's model can be rewritten as

$$q'' = \left\{ \frac{\rho_l i_{fg} k_l^3 \Delta T_s^3}{\mu_l} \left(\frac{C^4 \Delta \rho g}{L_g} + \frac{\sigma \left|\frac{d\kappa}{ds}\right|}{4L_s} \right) \right\}^{1/4} \tag{8}$$

where L_g and L_s are the condensing lengths influenced by gravity and surface tension, respectively. The coefficient C is chosen following Rose's (1994) model depending on what part of the tube is being modeled. For example, for the vertical plate with the rectangular-fin geometry, the condensation heat flux between the fins at their root (q_r'') is calculated as

$$q_r'' = \left(\frac{\rho_l i_{fg} k_l^3 \Delta T_s^3}{\mu_l}\right)^{1/4} \left(\frac{0.79 \Delta \rho g}{L_y}\right)^{1/4} \tag{9}$$

Equation (9) was obtained by neglecting surface tension drainage effects in the channel.

The fin-tip and the fin-side condensation are lumped into the condensation heat flux to the fin, while neglecting the effects of gravity, as

[4]The condensate curvature gradient is defined here as the change of the curvature of the liquid–vapor interface of the condensate with respect its own arc length (which is approximated by the fin length and zero at the center of the fin tip).

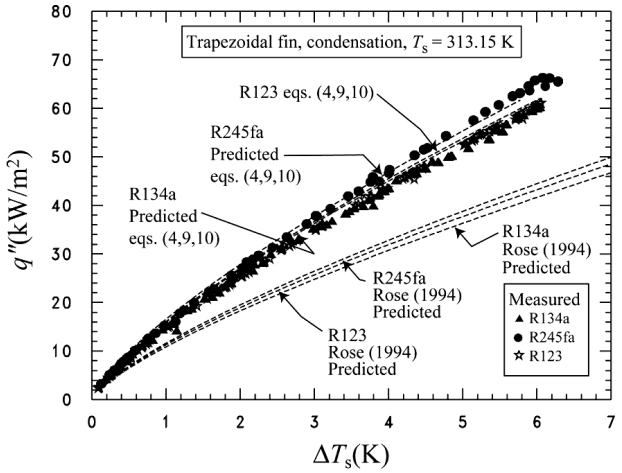

FIG. 7: Comparison between predicted and measured condensation heat fluxes for R134a, R245fa, and R123 on a trapezoidal surface.

$$q''_f = \left(\frac{\rho_l i_{fg} k_l^3 \Delta T_s^3}{\mu_l}\right)^{1/4} \left(\frac{\sigma\pi}{8e\,(2t_t)^2}\right)^{1/4} \qquad (10)$$

Neglecting gravity is a valid assumption for refrigerant condensation for most fin-length fin heights less than 1.5 mm (Kedzierski and Webb, 1990). Equation (10) was obtained by setting condensate curvature gradient on the fin to $\pi/[2(2t_t)^2]$ and the condensing length on the fin to the fin height, e. The curvature gradient is assumed to be concentrated at the corner of the fin-tip, as was also done by Adamek and Webb (1990) and Honda and Nozu (1987), and assumed to be constant. Webb et al. (1982) were some of the first researchers to apply a linear approximation for the curvature gradient on a fin. The difference between the curvature gradient approximation in the literature and that used in Eq. (10) is that the influence of the curvature gradient is assumed to be confined to twice the thickness of the fin tip, while the region for condensation heat transfer remains the entire fin height.[5]

Figure 7 compares the present condensation heat flux measurements for the trapezoidal plate to predictions using Eq. (4) with Eqs. (9) and (10). The predictions were done by setting c_b to zero as was done for the Rose (1994) predictions. In addition, the area ratio and the heat flux terms for the fin side and the fin tip were combined into a single term for both. Figure 7 shows that the modified Rose model predicts the driving temperature difference to within 0.4 K for all of the fluids and for the entire heat flux range. Evaluated at the same heat flux, the average difference between the measured and the predicted driving temperature difference was –0.08, –0.10, and 0.01 K for R134a, R123, and R245fa, respectively.

The Rose (1994) model was also modified to predict the Turbo-CII surface by developing a dimensional constant for the average curvature gradient normalized by an arbitrary condensing length for use in Eq. (8):

$$\frac{1}{L_s}\left|\frac{d\kappa}{ds}\right| = -1.34 \times 10^{12}\left[m^{-3}\right] \qquad (11)$$

Equation (11) was developed from a least-squares regression of the calculated curvature gradients for R134a and the R245fa condensation measurements on the Turbo-CII vertical plate.

When Eq. (11) is substituted into Eq. (8), while neglecting the gravity term, the average condensation heat flux based on the projected area for the Turbo-CII geometry on the vertical plate of this study is obtained and plotted in Fig. 8. Figure 8 shows that the modified Rose model, while using Eq. (11), predicts the driving temperature difference to within 1.2 K for R245fa and R134a for the entire heat flux range. Evaluated at the same heat flux, the average difference between the measured and the predicted driving temperature difference was 0.3 and –0.5 K for R134a and R245fa, respectively. For driving temperature differences increasing from near zero to 7 K, the heat flux for R123 is overpredicted from approximately 5% to 300% of the measured heat flux. The poor agreement between the model and the measured condensation heat transfer for R123 is likely due to partial flooding of the test surface.

The general model given in Eq. (4) along with Eq. (11) and Eq. (8) can be combined to develop an expression for predicting condensation on a Turbo-CII or Turbo-C tube:

$$q'' = \frac{0.683\,(1-c_b)}{p_f}\left(\frac{\xi\rho_l i_{fg} k_l^3 \Delta T_s^3 \sigma}{4\mu_l}\right)^{1/4} \qquad (12)$$

All fluid properties are evaluated at the saturated condition. The fin pitch (p_f) in the denominator of the first term of Eq. (12) accounts for surface area differences between tubes as caused by the fin pitch. The dimensional constant ξ is set to 1 m, which is required to ensure dimensional consistency between the leading constant (0.683) and the rest of the parameters in Eq. (12).

Figure 9 compares the predictions of Eq. (12) to the measurements of Jung et al. (1999) at a saturation tem-

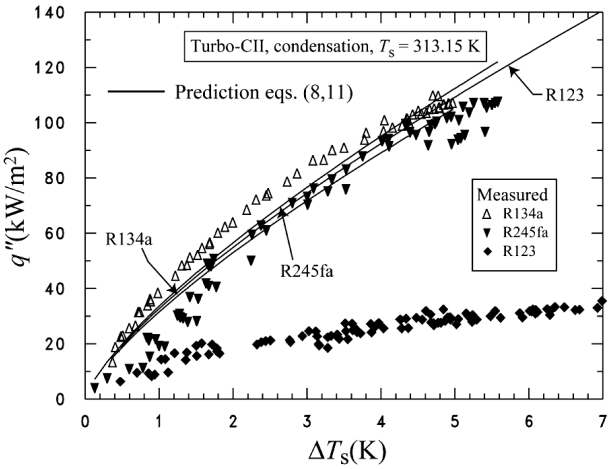

FIG. 8: Comparison between predicted and measured condensation heat fluxes for R134a, R245fa, and R123 on a Turbo-CII surface.

[5]For heights less than twice the fin-tip thickness, it is recommended to use e^3 rather than $e(2t_t)^2$ in the denominator of Eq. (10).

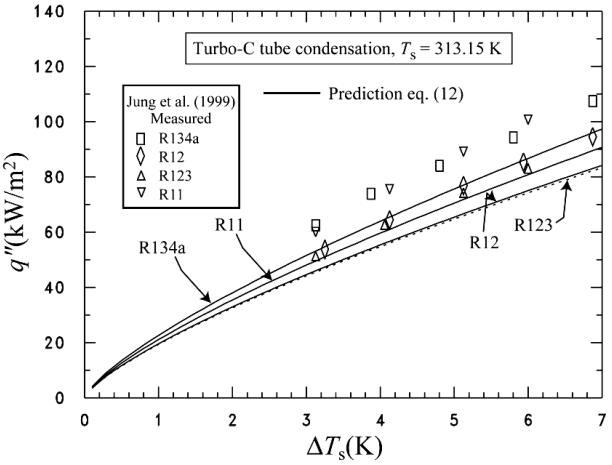

FIG. 9: Comparison between predicted and measured condensation heat fluxes for various refrigerants on the Turbo-C tube.

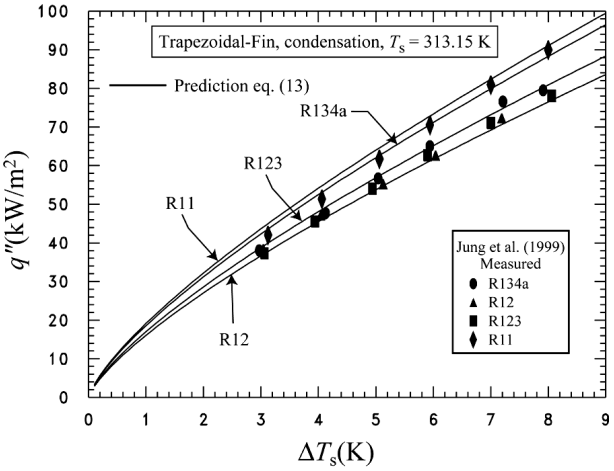

FIG. 10: Comparison between predicted and measured condensation heat fluxes for various refrigerants on the trapezoidal-finned tube.

perature of 312.15 K for an 18.9 mm diameter Turbo-C tube with 1654 fpm and an S_r of 0.25 mm. The predicted heat fluxes are within 15% of all the measured values for R11, R12, R123, and R134a.

A general condensation model for trapezoidal, low-finned tubes can be developed in a similar manner as was done for Eq. (12) by substituting Eqs. (9) and (10) into Eq. (4):

$$q'' = \frac{(1-c_b)}{p_f}\left(\frac{\rho_l i_{fg} k_l^3 \Delta T_s^3}{\mu_l}\right)^{1/4}\left\{(2e+S_r+t_t)\right.$$
$$\left.\times\left(\frac{\sigma\pi}{8e\,(2t_t)^2}\right)^{1/4}+\left(\frac{D_r S_r}{D_o}\right)\left(\frac{0.28\Delta\rho g}{D_r}\right)^{1/4}\right\} \quad (13)$$

Here, the area ratios of the tube have been estimated with previously defined fin and tube parameters. The constant 0.28 for round, horizontal tubes (C_t^4) was used in Eq. (13) to represent condensation between the fins rather than using the constant 0.79 that was used for vertical plates in Eq. (9).

Figure 10 compares the predictions of Eq. (13) to the measurements of Jung et al. (1999) at a saturation temperature of 312.15 K for an 18.9 mm diameter trapezoidal-finned tube with 1024 fpm, e = 1.124 mm, t_t = 0.252 mm, and an S_r of 0.4 mm. As shown in Fig. 10, the predicted heat fluxes for R123, R12, and R11 are within 7% of all the measured values. The heat flux for R134a is overpredicted by roughly 10%.

7. CONCLUSIONS

Vapor-space condensation heat transfer data for pure R123, R134a, and R245fa were measured on two vertical plates: one with the integral trapezoidal-fin surface and the other with the Turbo-CII surface. The condensation heat flux of the Turbo-CII, based on the projected area, was approximately double that of the trapezoidal-fin surface. The condensation heat flux of R134a and R245fa on the Turbo-CII surface were similar, being within 18 kW/m^2 of each other. The condensation heat flux for R123 on the Turbo-CII surface was between 10 and 80 kW/m^2 less than that of R245fa. It is believed that the poor performance of R123 on the Turbo-CII was due to partial flooding of the fins. The heat flux for the trapezoidal fin surface proved to be relatively insensitive to test refrigerant, being within approximately 8 kW/m^2 of each other for the same driving temperature difference.

An existing finned tube condensation model was modified to be expressed in terms of the gradient of the condensate curvature with respect to the length of the liquid–vapor interface. Expressions for the curvature gradients for the trapezoidal fin and the Turbo-CII surface were developed from the vertical plate data and used to modify the existing model. The modified model for the condensation on a vertical, trapezoidal-fin surface predicted the measured driving temperature difference to within 0.4 K and for all test fluids. Similarly, the modified model for the condensation on a vertical, Turbo-CII surface predicted the measured driving temperature difference to

within 1.2 K for R134a and R245fa. Using the curvature gradient derived for the Turbo-CII vertical plate data, a simple model was developed to predict the performance of a single Turbo-C or Turbo-CII tube. Measured heat fluxes from the literature were predicted to within 15% for four different fluids on a Turbo-C tube. The same concept was used to develop a model for condensation on trapezoidal, low-fin tubes. The model predicted data from the literature for four different fluids to within approximately 10% of the measurement.

ACKNOWLEDGMENTS

This work was jointly funded by NIST and the US Navy. The authors would also like to express appreciation to NIST personnel Glen Glaeser for his help with rig modifications, and to Kyongmin Kwon, Piotr Domanski, and Andrew Persily for their constructive review. We are also grateful for the review comments of Ki-Jung Park of the Korea Atomic Energy Research Institute. Thanks goes to Weiland Products for donating the trapezoidal fin surface and to Wolverine Tube for donating a Turbo-CII tube.

REFERENCES

Adamek, T. and Webb, R. L., Prediction of the film condensation on horizontal integral-fin tubes, *Int. J. Heat Mass Transf.*, vol. **33**, no. 8, pp. 1721–1735, 1990.

Brown, J. S., Introduction to alternatives for high-GWP HFC refrigerants, in *Proc. of ASHRAE/NIST Refrigerants Conf.*, Gaithersburg, MD, 2012.

Brown, J.S., Zilio, C., Brignoli, R., and Cavallini, A., Heat transfer and pressure drop penalization terms (exergy losses) during flow boiling of refrigerants, *Int. J. Energy Res.*, 2012.

Calm, J. M., Refrigerant Transitions . . . Again, in *Proc. of ASHRAE/NIST Refrigerants Conf.*, Gaithersburg, MD, 2012.

Carr, M. A., Experimental and Theoretical Study of Surface Tension Effects on Extended Surface Condensation, PhD Thesis, Catholic University of America, Washington, DC, 2002.

Cavallini, A., Brown, J. S., Del Col, D. and Zilio, C., In-tube condensation performance of refrigerants considering penalization terms (exergy losses) for heat transfer and pressure drop, *Int. J. Heat Mass Transf.*, vol. **53**, nos. 13–14, pp. 2885–2896, 2010.

Copenhagen Amendment, *The Amendment to the Montreal Protocol Agreed by the Fourth Meeting of the Parties*, United Nations Environment Programme, Nairobi, Kenya, United Nations (UN), New York, 1992.

European Mobile Directive, Directive 2006/40/EC of The European Parliament & of the Council of 17 May 2006 Relating to Emissions from Air-Conditioning Systems in Motor Vehicles & Amending Council Directive 70/156/EC, *Official Journal of the European Union*, 49(L 161), pp. 12–18, 2006.

Honda, H. and Nozu, S., A prediction method for heat transfer during film condensation on horizontal low integral-fin tubes, *ASME J. Heat Transf.*, vol. **109**, pp. 218–225, 1987.

Incropera, F. P. and DeWitt, D. P., *Fundamentals of Heat and Mass Transfer*, 5th ed., John Wiley & Sons, New York, 2002.

IPCC, *Climate Change 2007: The Physical Science Basis. Contribution of Working Group I to the Fourth Assessment Report of the Intergovernmental Panel on Climate Change*, Cambridge University Press, Cambridge, 2007.

Jung, D., Kim, C., Cho, S., and Song, K., Condensation heat transfer coefficients of enhanced tubes with alternative refrigerants for CFC11 and CFC12, *Int. J. Refrig.*, vol. **22**, pp. 548–557, 1999.

Kedzierski, M. A., *Calorimetric and Visual Measurements of R123 Condensation on Four Enhanced Surfaces*, NISTIR 5732, US Department of Commerce, Washington, DC, 1995.

Kedzierski, M. A., The effect of a boiling additive on R123 condensation on a vertical integral-fin surface, *Int. J. Refrig.*, vol. **23**, pp. 101–111, 2000.

Kedzierski, M. A. and Webb, R. L., Practical fin shapes for surface-tension-drained condensation, *J. Heat Transf.*, vol. **112**, pp. 479–485, 1990.

Kyoto Protocol, *United Nations Framework Convention on Climate Change*, United Nations (UN), New York, 1997.

Montreal Protocol, *Montreal Protocol on Substances that Deplete the Ozone Layer*, United Nations (UN), New York (1987 with subsequent amendments), 1987.

Nusselt, W., Die Oberflachenkondensation des Wasserdampfes, *Z. Ver. Deut. Ing.*, vol. **60**, pp. 541–546, 1916.

Park, K., Kang, D. G., and Jung, D., Condensation heat transfer coefficients of HFC245fa on a horizontal plain tube, *J. Mech. Sci. Technol.*, vol. **24**, no. 9, pp. 1911–1917, 2010.

Rohsenow, W. M., Webber, J. H., and Ling, A. T., Effect of vapor velocity on laminar and turbulent-film condensation, *Trans. ASME*, vol. **78**, pp. 1637–1644, 1956.

Rose, J. W., An approximate equation for the vapour-side heat-transfer coefficient for condensation on low-finned tubes, *Int. J. Heat Mass Transf.*, vol. **37**, no. 5, pp. 865–875, 1994.

Rudy, T. M., and Webb, R. L., Condensate retention on horizontal integral-fin tubes, *ASME J. Heat Transf.*, vol. **107**, no. 2, pp. 361–368, 1985.

Webb, R. L., Keswani, S. T., and Rudy, T. M., Investigation of surface tension and gravity effects in film condensation, in *Proc. of 7th Intl. Heat Transfer Conf.*, vol. 5, Munich, Hemi-

sphere Publishing, Washington, DC, pp. 175–180, 1982.

Webb, R. L., Rudy, T. M., and Kedzierski, M. A., Prediction of the condensation coefficient on horizontal integral-fin tubes, *J. Heat Transf.*, vol. **107**, pp. 369–376, 1985.

Zener, C. and Lavi, A., Drainage systems for condensation, *ASME J. Eng. Power*, vol. **96**, pp. 209–215, 1973.